

Isotope shifts due to the $1s^22s\ ^2S_{1/2} \rightarrow 1s^22p\ ^2P_{1/2,3/2}$ transitions of Li-like Th^{87+} ions

Huqiang Lu(路虎强), Bingbing Li(李兵兵), Mingye Yang(杨明叶), Lin Dong(董霖), Yanmin Wang(王雁敏), Maijuan Li(李麦娟), Lei Wu(吴磊), Jiguang Li(李冀光), Jun Jiang(蒋军), Chenzhong Dong(董晨钟), and Denghong Zhang(张登红)

Citation: Chin. Phys. B, 2025, 34 (**7**): 073203. DOI: 10.1088/1674-1056/adcb21
http://cpb.iphy.ac.cn; http://iopscience.iop.org/cpb

What follows is a list of articles you may be interested in

Steering the energy sharing of electrons in nonsequential double ionization with orthogonally polarized two-color field

Guangqi Fan(樊光琦), Zhijie Yang(杨志杰), Fenghao Sun(孙烽豪), Jinmei Zheng(郑金梅), Yuntian Han(韩云天), Mingqian Huang(黄明谦), and Qingcao Liu(刘情操)

Chin. Phys. B, 2024, 33 (**8**): 083102. DOI: 10.1088/1674-1056/ad4bc0

Energy levels and magnetic dipole transition parameters for the nitrogen isoelectronic sequence

Mu-Hong Hu(胡木宏), Nan Wang(王楠), Pin-Jun Ouyang(欧阳品均),Xin-Jie Feng(冯新杰), Yang Yang(杨扬), and Chen-Sheng Wu(武晨晟)

Chin. Phys. B, 2022, 31 (**9**): 093101. DOI: 10.1088/1674-1056/ac7a12

Theoretical calculations of hyperfine splitting, Zeeman shifts, and isotope shifts of $^{27}Al^+$ and logical ions in Al^+ clocks

Xiao-Kang Tang(唐骁康), Xiang Zhang(张祥), Yong Shen(沈咏), and Hong-Xin Zou(邹宏新)

Chin. Phys. B, 2021, 30 (**12**): 123204. DOI: 10.1088/1674-1056/ac0130

Calculations of atomic polarizability for beryllium using MCDHF method

Hui Dong(董辉), Jun Jiang(蒋军), Zhongwen Wu(武中文), Chenzhong Dong(董晨钟), and Gediminas Gaigalas

Chin. Phys. B, 2021, 30 (**4**): 043103. DOI: 10.1088/1674-1056/abd92d

Theoretical investigation on forbidden transition properties of fine-structure splitting in ^2D state for K-like ions with $26 \le Z \le 36$

Jian-Peng Liu(刘建鹏), Cheng-Bin Li(李承斌), Hong-Xin Zou(邹宏新)

Chin. Phys. B, 2017, 26 (**10**): 103201. DOI: 10.1088/1674-1056/26/10/103201

Isotope shifts due to the $1s^22s\ ^2S_{1/2} \rightarrow 1s^22p\ ^2P_{1/2,3/2}$ transitions of Li-like Th^{87+} ions

Huqiang Lu(路虎强)[1], Bingbing Li(李兵兵)[1], Mingye Yang(杨明叶)[3], Lin Dong(董霖)[1], Yanmin Wang(王雁敏)[1], Maijuan Li(李麦娟)[1], Lei Wu(吴磊)[1], Jiguang Li(李冀光)[3,†], Jun Jiang(蒋军)[1,‡], Chenzhong Dong(董晨钟)[1], and Denghong Zhang(张登红)[1,2,§]

[1] *Key Laboratory of Atomic and Molecular Physics and Functional Materials of Gansu Province, College of Physics and Electronic Engineering, Northwest Normal University, Lanzhou* 730070, *China*

[2] *Department of Physics, Tianshui Normal University, Tianshui* 741000, *China*

[3] *High Energy Density Physics, Institute of Applied Physics and Computational Mathematics, Beijing* 100088, *China*

(Received 27 February 2025; revised manuscript received 31 March 2025; accepted manuscript online 10 April 2025)

The transition energies of the $1s^22s\ ^2S_{1/2} \rightarrow 1s^22p\ ^2P_{1/2,3/2}$ transitions in Li-like Th^{87+} ions were calculated by combining the multi-configuration Dirac–Hartree–Fock (MCDHF) method with the model-quantum electrodynamics (model-QED) approach. The effects of electron correlation, Breit interaction, and QED effects were analyzed in detail. The isotope shifts, including the mass shifts and field shifts, due to the $2s\ ^2S_{1/2} \rightarrow 2p\ ^2P_{1/2,3/2}$ transitions were then calculated using two different methods, namely, the MCDHF method and the finite-field method. The results show that these two methods are in excellent agreement.

Keywords: isotope shift, MCDHF method, finite-field method, QED effect

PACS: 31.15.V–, 31.15.am, 31.30.J–, 31.30.Gs

DOI: 10.1088/1674-1056/adcb21 **CSTR:** 32038.14.CPB.adcb21

1. Introduction

Theoretical and experimental studies of isotope shifts, including field shifts and mass shifts (MSs), in highly charged ions provide a means of testing quantum electrodynamics (QED) theory. Furthermore, these studies serve as an excellent tool for precisely determining differences in nuclear charge radius among isotopes.[1] For instance, the relativistic mass-shift operator and its QED correction (including vacuum polarization (VP) and self-energy correction (SE)) for medium- and high-Z systems have been effectively tested through high-precision measurements of isotope shifts for B-like argon[2] and Li-like neodymium.[3] The nuclear charge radius of Na-like Xe ions in a high charge state was determined with high precision using extreme ultraviolet (EUV) spectroscopy, as reported in Refs. [4–6].

Thorium is a crucial element in the fields of nuclear energy and high-precision measurement physics. The nucleus of the ^{229}Th isotope exhibits extremely low energy excitation, with an estimated value of approximately 8.338 (24) eV.[7,8] Currently, a considerable number of researchers are engaged in the development of high-precision nuclear clocks.[9–12] Therefore, it is essential to understand the isotope shifts of highly charged thorium ions to analyze atomic structure and nuclear parameters in these experiments. The field shifts and MSs the Li-like Th^{87+} ion were calculated by Zubova *et al.*[13] using a combination of perturbation methods and the configuration-interaction Dirac–Fock–Sturm (CI-DFS) method, taking into account the effects of electronic correlations, the Breit effect, and QED corrections. The MSs and field shifts of the $1s^22s\ ^2S_{1/2} \rightarrow 1s^22p\ ^2P_{1/2,3/2}$ transitions of the Li-like Th^{87+} ion were also calculated by Li *et al.*[14] using the multi-configuration Dirac–Hartree–Fock (MCDHF) method, with inclusion of electronic correlations and the Breit effect. Significant discrepancies were observed between these two calculations. For instance, the normal mass shift (NMS) for the $1s^22s\ ^2S_{1/2} \rightarrow 1s^22p\ ^2P_{1/2}$ transition calculated by Zubova *et al.*[13] differs from the results of Li *et al.*[14] by approximately 10%. A similar 10% discrepancy exists in the field shifts. Therefore, to understand these discrepancies, further detailed studies are required.

In this work, the wavefunctions and energy levels of the $1s^22s\ ^2S_{1/2}$ and $1s^22p\ ^2P_{1/2,3/2}$ transitions of Li-like Th^{87+} ions are calculated using the MCDHF method and the GRASP2018 package.[15,16] The model-QED method[17–19] is used to calculate the contributions of QED effects. Furthermore, two different methods, namely, the MCDHF and finite-field methods, are employed to calculate the isotope shifts of the $1s^22s\ ^2S_{1/2} \rightarrow 1s^22p\ ^2P_{1/2,3/2}$ transitions in Li-like Th^{87+} ions. The results show that the isotope shifts calculated by

†Corresponding author. E-mail: li_jiguang@iapcm.ac.cn
‡Corresponding author. E-mail: jiangjun@nwnu.edu.cn
§Corresponding author. E-mail: zhangdh@nwnu.edu.cn

© 2025 Chinese Physical Society and IOP Publishing Ltd. All rights, including for text and data mining, AI training, and similar technologies, are reserved.

these two methods are in good agreement.

2. Theory and computational methodology

2.1. MCDHF method

The wave functions and energy levels of Li-like Th^{87+} are calculated using the MCDHF method and the corresponding GRASP2018 package.[15,16] A detailed description of the MCDHF method can be found in Refs. [20–22]. Here, only a brief description is given. The atomic state wave functions (ASFs) are described according to the MCDHF method as linear combinations of configuration state wave functions (CSFs) with the same parity P, total angular momentum J, and its z-component M_J, i.e., the ASFs are written as

$$\Psi(\gamma PJM_J) = \sum_{v=1}^{N} c_v \Phi(\gamma_v PJM_J), \tag{1}$$

where c_v is the mixing coefficient, and γ and γ_v represent all additional quantum numbers. The configuration wave function consists of a linear combination of the Slater determinants of the single-electron orbital wave functions. The single-electron orbitals and the mixing coefficients are optimized simultaneously in the SCF procedure. The Breit interaction and QED corrections are included in the subsequent relativistic configuration (RCI), where only mixing coefficients are variable. The calculation is performed using the GRASP 2018 package.[15,16]

In this study, the model-QED approach is adopted to estimate the QED corrections as well, which is expressed by the operator as[17–19]

$$H^{\mathrm{QED}} = h^{\mathrm{SE}} + V_{\mathrm{Uehl}} + V_{\mathrm{WK}}, \tag{2}$$

where h^{SE} is SE, V_{Uehl} is the Uehling potential, V_{WK} is the Wichmann–Kroll (WK) potential, the sum of V_{Uehl} and V_{WK} gives the VP, and h^{SE} can be classified as a local and nonlocal sum such that

$$h^{\mathrm{SE}} = h^{\mathrm{SE}}_{\mathrm{loc}} + h^{\mathrm{SE}}_{\mathrm{nloc}}, \tag{3}$$

where $h^{\mathrm{SE}}_{\mathrm{loc}}$ and $h^{\mathrm{SE}}_{\mathrm{nloc}}$ represent the quasi-local operator and nonlocal operator, respectively.

2.2. Isotope shift

The isotope shift consists of two parts: the field shift, which is a consequence of nuclear charge distributions, and the MS, which is a result of the different finite nuclear masses. The isotope shift of the same energy level i between two isotopes with mass numbers $A > A'$ can be expressed as the sum of the MS $\delta E^{A,A'}_{i,\mathrm{MS}}$ and the field shift $\delta E^{A,A'}_{i,\mathrm{FS}}$

$$\delta E^{A,A'}_{i,\mathrm{IS}} = \delta E^{A,A'}_{i,\mathrm{MS}} + \delta E^{A,A'}_{i,\mathrm{FS}}. \tag{4}$$

The MS can be written as[23–26]

$$\begin{aligned}&\delta E^{A,A'}_{i,\mathrm{MS}}\\ &= \delta E^{A,A'}_{i,\mathrm{NMS}} + \delta E^{A,A'}_{i,\mathrm{SMS}} = \left(\frac{M'-M}{MM'}\right)(K_{i,\mathrm{NMS}} + K_{i,\mathrm{SMS}}),\end{aligned} \tag{5}$$

where $\delta E^{A,A'}_{i,\mathrm{NMS}}$ is the NMS, $\delta E^{A,A'}_{i,\mathrm{SMS}}$ is the special mass shift (SMS), M is the mass number of isotope A, and M' is the mass number of isotope A'. $K_{i,\mathrm{NMS}}$ and $K_{i,\mathrm{SMS}}$ denote the NMS and SMS parameters obtained under the lowest-order approximation:

$$\begin{aligned}K_{i,\mathrm{NMS}} &= M\langle\Psi_i(\gamma PJM_J)|\hat{H}_{\mathrm{NMS}}|\Psi_i(\gamma PJM_J)\rangle,\\ K_{i,\mathrm{SMS}} &= M\langle\Psi_i(\gamma PJM_J)|\hat{H}_{\mathrm{SMS}}|\Psi_i(\gamma PJM_J)\rangle.\end{aligned} \tag{6}$$

Here, $\hat{H}_{\mathrm{NMS}}$ and $\hat{H}_{\mathrm{SMS}}$ are the Hamiltonian quantities of the NMS and the SMS, respectively, given by

$$\begin{aligned}\hat{H}_{\mathrm{NMS}} &= \frac{1}{2M}\sum_{i=1}^{N}\left\{\boldsymbol{p}_i^2 - \frac{\alpha Z}{r_i}\left[\boldsymbol{\alpha}_i + \frac{\alpha Z}{r_i}\frac{(\boldsymbol{\alpha}_i\cdot\boldsymbol{r}_i)\boldsymbol{r}_i}{r_i^2}\right]\cdot\boldsymbol{p}_i\right\},\\ \hat{H}_{\mathrm{SMS}} &= \frac{1}{2M}\sum_{i\neq j}^{N}\left\{\boldsymbol{p}_i - \frac{\alpha Z}{r_i}\left[\boldsymbol{\alpha}_i + \frac{(\boldsymbol{\alpha}_i\cdot\boldsymbol{r}_i)\boldsymbol{r}_i}{r_i^2}\right]\right\}\cdot\boldsymbol{p}_j,\end{aligned} \tag{7}$$

where $\boldsymbol{r}$ is the position vector, $\boldsymbol{\alpha}_i$ is the Dirac matrix, α is the fine structure constant, Z is the nuclear charge number, M is the nuclear mass number, $\boldsymbol{p}_i$ is the momentum operator for the ith electron, and $\boldsymbol{p}_j$ is the momentum operator for the jth electron. The MS of the transition i between two energy levels u and l is expressed as

$$\delta\nu^{AA'}_{i,\mathrm{MS}} = \left(\frac{M'-M}{MM'}\right)\frac{\Delta K_{\mathrm{MS}}}{h}, \tag{8}$$

where $\Delta K_{\mathrm{MS}} = (K_{u,\mathrm{MS}} - K_{l,\mathrm{MS}})$ is the MS parameter between the two energy levels u and l. The field shift factor in Eq. (4) is written as[27]

$$F = \frac{Z}{3\hbar}\left(\frac{e^2}{4\pi\varepsilon_0}\right)\Delta|\Psi(0)|^2. \tag{9}$$

The F is proportional to the amount of variation $\Delta|\Psi(0)|^2$ in the total probability density amplitude of electrons at the origin, and $\Delta\mid\Psi(0)\mid^2 = \rho^e_u(0) - \rho^e_l(0)$, $\rho^e(0) = \langle\Psi|\sum_i r_i|\Psi\rangle$. The field shift of the transition i between two energy levels u and l is expressed as

$$\delta\nu^{A,A'}_{i,\mathrm{FS}} \approx \Delta F_i \delta\left\langle r^2\right\rangle^{A,A'}. \tag{10}$$

That is, the isotope shift can finally be written as

$$\delta E^{A,A'}_{i,\mathrm{IS}} = \left(\frac{M'-M}{MM'}\right)K_{i,\mathrm{MS}} + \delta\left\langle r^2\right\rangle^{A,A'}F_i. \tag{11}$$

Therefore, when the isotope shift $\delta E^{A,A'}_{i,\mathrm{IS}}$ is measured experimentally, we can accurately obtain $\delta\left\langle r^2\right\rangle^{A,A'}$, once the mass- and field-shift factors are determined by atomic-structure calculations.

3. Results and discussion

3.1. Transition energy

In the present work, the active space method is used to consider electron correlation effects for the $1s^22s$ and $1s^22p$ states. First, we optimized the 1s, 2s and 2p occupied orbitals separately for two states with different parities in the Dirac–Hartree–Fock (DHF) approximation. The CSFs are then generated by single and double (SD) excitations to correlation orbitals from the occupied orbitals. The correlation orbitals are augmented layer by layer, which makes it possible to monitor the convergence of physical quantities related to the expansion of the configuration space. After that, the SCF calculation is performed separately to minimize the energy eigenvalue of each state. The correlation orbital set is restricted to the principal quantum numbers $n = 2,3,\ldots,7$, and the orbital quantum numbers $l \leq 5$.

Figure 1 shows the convergence of the energy eigenvalues for the $1s^22s\ ^2S_{1/2}$ and $1s^22p\ ^2P_{1/2,3/2}$ states of Li-like Th^{87+} ions. We can see that electron correlation effects converge rapidly due to the rational selection of the calculation model. The energy values converge to −10301.77, −10291.61, and −10151.98 (a.u.) for the $1s^22s\ ^2S_{1/2}$, $1s^22p\ ^2P_{1/2}$, and $1s^22p\ ^2P_{3/2}$ states, respectively.

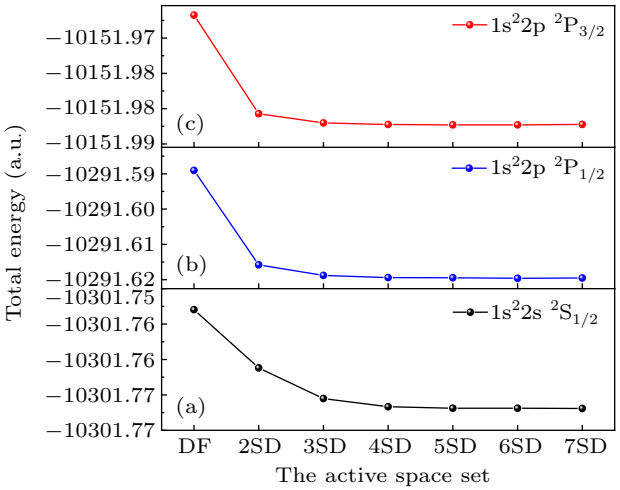


Fig. 1. The convergence of the eigenvalues (in a.u.) for Li-like Th^{87+} ions in the $1s^22s\ ^2S_{1/2}$ and $1s^22p\ ^2P_{1/2,3/2}$ states as a function of the expanded space. DF denotes the DHF calculations, while nSD ($n = 2, 3,\ldots, 7$) indicates calculations that consider SD excitations into the corresponding correlation orbitals. n is the highest principal quantum number of the correlation orbitals.

Table 1 lists the contributions of the Breit interactions and QED effects to the transition energy of the $1s^22s\ ^2S_{1/2} \rightarrow 1s^22p\ ^2P_{1/2,3/2}$ transitions, while the final total value is determined using the model-QED computational approach. Meanwhile, the QED corrections obtained using the two calculation methods show good agreement. These results were compared with some available theoretical results.[28–34] The results obtained in this study are in good agreement with those given in Refs. [28,30–32]. In addition, it should be noted that the contributions of the Breit effect and the QED effect to the transition energies for the $1s^22s\ ^2S_{1/2} \rightarrow 1s^22p\ ^2P_{1/2}$ transitions are 33.70 eV and −39.17 eV, respectively. Since these contributions have opposite signs, they nearly cancel each other out. In contrast, for the transitions $1s^22s\ ^2S_{1/2} \rightarrow 1s^22p\ ^2P_{3/2}$, the contributions from the Breit effect and the QED effect have the same signs, with values of −13.09 eV and −36.93 eV, respectively. Our results closely agree with experimental results,[34] with only a 0.01% difference.

Table 1. Contributions of the Breit effect and the QED effect to the transition energy (in eV) of Li-like Th^{87+} ions $1s^22s\ ^2S_{1/2} \rightarrow 1s^22p\ ^2P_{1/2,3/2}$. CI stands for the configuration-interaction results, QED^1 stands for the QED correction calculated by the GRASP 2018 package, and QED^2 stands for the QED correction obtained with the model-QED approach.

	$1s^22s\ ^2S_{1/2} \rightarrow 1s^22p\ ^2P_{1/2}$		$1s^22s\ ^2S_{1/2} \rightarrow 1s^22p\ ^2P_{3/2}$	
	This work	Refs.	This work	Refs.
CI	276.17	275.95[28]	4075.80	4075.56[28]
Breit	33.70	33.25[28]	−13.09	−14.12[28]
				−14.14[29]
QED^1	−38.94		−37.66	
QED^2	−39.17	−38.50[28]	−36.93	−36.44[28]
		−39.68[30]		−36.09[29]
		−38.45[31]		−35.87[31]
		−38.54[32]		−36.08[32]
Total	270.70	270.80[28]	4025.78	4025.11[28]
		270.60[30]		4025.10[31]
		270.72[31]		4025.25[32]
		270.74[32]		4028.60[33]
		270.29[33]		
Expt.				4025.23 ± 0.14[34]

3.2. Isotope shift parameters calculated using the MCDHF method

The isotope shift parameters are calculated using the RIS4 program.[35] Figure 2 shows the convergence of the NMS parameter ($K_{i,\mathrm{NMS}}$), the SMS parameter ($K_{i,\mathrm{SMS}}$), and the MS

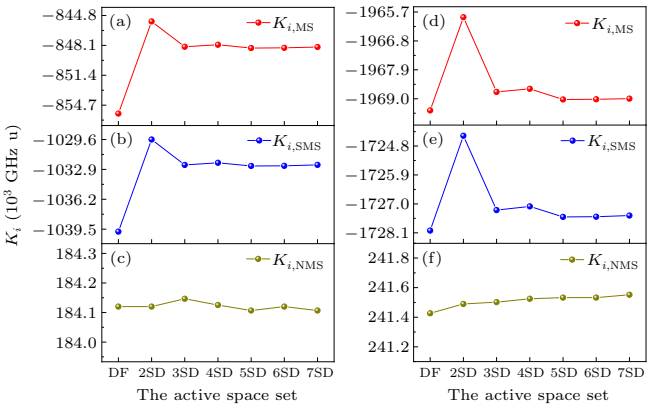


Fig. 2. The convergence of $K_{i,\mathrm{NMS}}$, $K_{i,\mathrm{SMS}}$, and $K_{i,\mathrm{MS}}$ (in 10^3 GHz u) for Li-like Th^{87+} ions $1s^22s\ ^2S_{1/2} \rightarrow 1s^22p\ ^2P_{1/2}$ transitions (panels (a)–(c)) and $2s\ ^2S_{1/2} \rightarrow 2p\ ^2P_{3/2}$ transitions (panels (d)–(f)) as the extended space changes. DF denotes the DHF calculations, while nSD (n is the highest principal quantum number of correlation orbitals) represents the multi-configuration calculations with the SD excitations into the correlation orbitals.

Table 2. Contributions of Breit interactions and QED effects to $K_{i,\mathrm{NMS}}$, $K_{i,\mathrm{SMS}}$, and $K_{i,\mathrm{MS}}$ (in units of 10^3 GHz u) for the $1s^22s\ ^2S_{1/2} \rightarrow 1s^22p\ ^2P_{1/2,3/2}$ transition of Li-like Th^{87+} ions. DF denotes the single-configuration calculations, RCI refers to the multi-configuration calculations, RCI + Breit includes the Breit interactions, and RCI + Breit + QED indicates the value obtained by adding the QED nuclear recoil corrections.

	$1s^22s\ ^2S_{1/2} \rightarrow 1s^22p\ ^2P_{1/2}$					
	$K_{i,\mathrm{NMS}}$		$K_{i,\mathrm{SMS}}$		$K_{i,\mathrm{MS}}$	
	This work	Refs.	This work	Refs.	This work	Refs.
DF	184.14		−1039.77		−855.63	−846.50[14]
RCI	184.13	175.7[13]	−1032.40	−1033.4[13]	−848.28	−847.20[14]
RCI + Breit	172.25		−1001.33		−829.08	−783.20[14]
						−857.70[13]
QED						−2583[36]
RCI + Breit + QED					−3412.08	−3441[13]
	$1s^22s\ ^2S_{1/2} \rightarrow 1s^22p\ ^2P_{3/2}$					
	$K_{i,\mathrm{NMS}}$		$K_{i,\mathrm{SMS}}$		$K_{i,\mathrm{MS}}$	
	This work	Refs.	This work	Refs.	This work	Refs.
DF	−241.43		−1728.02		−1969.44	−1977.00[14]
RCI	−241.55	−240.9[13]	−1727.44	−1731.6[13]	−1969.00	−1970.00[14]
RCI + Breit	−263.37		−1701.58		−1964.95	−1896.00 [14]
						−1972.50[13]
QED						−2441[36]
RCI + Breit + QED					−4405.95	−4416[13]

parameter ($K_{i,\mathrm{MS}}$) for the transitions $1s^22s\ ^2S_{1/2} \rightarrow 1s^22p\ ^2P_{1/2}$ (Figs. 2(a)–2(c)) and $1s^22s\ ^2S_{1/2} \rightarrow 1s^22p\ ^2P_{3/2}$ (Figs. 2(d)–2(f)). It can be seen that the impact of electronic correlation effects on $K_{i,\mathrm{SMS}}$ is significant, resulting in a substantial impact on the total MSs $K_{i,\mathrm{MS}}$. In contrast, the impact on $K_{i,\mathrm{NMS}}$ is relatively minor. As the active space increases, these parameters show good convergence.

Table 2 shows the contributions of the Breit interactions and QED effects to the MS parameters. It can be found that our results for the DF and RCI calculations are in good agreement with those of Li *et al.*[14] However, when the contributions of the Breit interaction are considered, there is a discrepancy of approximately 6% between our $K_{i,\mathrm{MS}}$ results for the transitions $1s^22s\ ^2S_{1/2} \rightarrow 1s^22p\ ^2P_{1/2}$ and those of Li *et al.*[14] Our results are in good agreement with those calculated by Zubova *et al.*[13] In addition, we should mention that for highly charged ions, the contribution of QED to the nuclear recoil operator is significantly enhanced.[13,36] In our calculations, the model-QED method is used to obtain the QED effects on the wave functions and energy levels. However, the QED correction to the nuclear recoil operator is not included. In this study, we added the QED contributions from Refs. [13,36] into our final results. The final results are in good agreement with those of Zubova *et al.*,[13] with a discrepancy of less than 1%. It should be noted that there is no experimental data that can be directly compared, which makes the mutual consistency between these theoretical calculations particularly important. Future experimental measurements are crucial to further verify the accuracy of different theoretical models dealing with Breit interaction and QED modification.

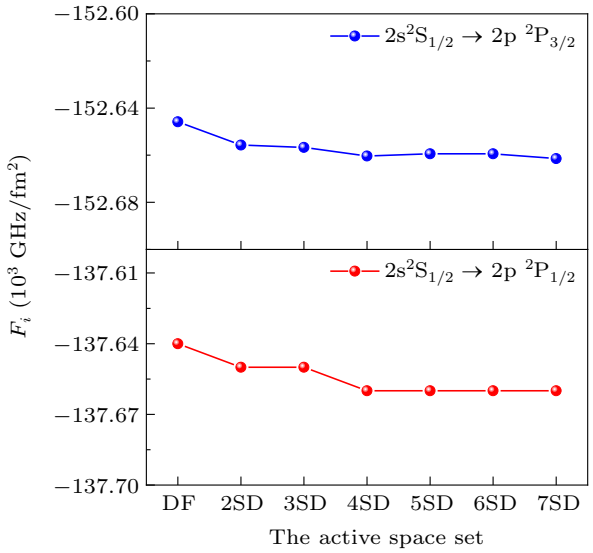


Fig. 3. The trends of the transition rates F_i (in units of 10^3 GHz/fm^2) for the Li-like Th^{87+} ions transitions $2s\ ^2S_{1/2} \rightarrow 2p\ ^2P_{1/2,3/2}$ as the extended space changes. DF indicates the parameter values without any excitation, while nSD ($n = 2, 3, \ldots, 7$, n is the highest principal quantum number) represents the parameter values corresponding to SD excitations into their respective correlation orbitals.

Figure 3 shows the convergence of the field shift parameter F_i for the transition $1s^22s\ ^2S_{1/2} \rightarrow 1s^22p\ ^2P_{1/2,3/2}$ (in 10^3 GHz/fm^2). It can be seen that the influence of electronic correlation effects on F_i is very small. For the calculation of the field shift parameters, we first computed the configuration-interaction wave functions, which provided the dominant contribution to the parameters. Subsequently, by calculating the "CI+Breit" and "CI+Breit+QED" wave functions, we derived the incremental contributions of the Breit effect and the QED effect to the field shift parameters. Table 3 shows the contributions of the Breit effect and the QED effect to the field shift

parameter F_i; the contributions of the Breit effect and QED effect to F_i are less than 1%. Moreover, our results for F_i are in excellent agreement with the results obtained by Zubova *et al.*[13] After adding the QED effect, our calculated F_i for the $1s^22s\ ^2S_{1/2} \rightarrow 1s^22p\ ^2P_{1/2,3/2}$ transition corresponds very well with the result of Zubova *et al.*,[13] with a difference of less than 5%. Our result shows a difference of about 10% in the field-shift factor for the $1s^22s\ ^2S_{1/2} \rightarrow 1s^22p\ ^2P_{1/2}$ transition compared to that of Li *et al.*[14] This is due to the different nuclear parameters used in the calculations. The main difference is in the Fermi distribution parameter c, which is calculated as 7.03 in our work but has a value of 6.93 in Li *et al.*'s[14] calculation.

Table 3. Contributions of Breit interactions and QED effects to F_i (in units of 10^3 GHz/fm^2) for the $1s^22s\ ^2S_{1/2} \rightarrow 1s^22p\ ^2P_{1/2,3/2}$ transition of Li-like Th^{87+} ions.

	$1s^22s\ ^2S_{1/2} \rightarrow 1s^22p\ ^2P_{1/2}$			$1s^22s\ ^2S_{1/2} \rightarrow 1s^22p\ ^2P_{3/2}$		
	This work	Ref. [14]	Ref. [13]	This work	Ref. [14]	Ref. [13]
DF	−137.64	−151.20	−137.64	−152.65	−169.00	−152.65
RCI	−137.66	−152.10	−137.65	−152.66	−168.50	−151.86
RCI + Breit	−132.18	−151.80	−136.98	−148.18	−168.10	−151.86
RCI + Breit + QED	−136.98		−136.25	−156.21		−150.79

3.3. Isotope shift parameters calculated using the finite-field method

We then used the finite-field method to extract isotope shift factors from the eigenvalues. In these calculations, we used the RCI method, incorporating the approach of Yang, Jönsson, Li, *et al.* (in preparation), to obtain the energy eigenvalues. The orbital set used here is the same as that used in the MCDHF calculations above. In the finite-field method, the MS operator is added to the many-particle Hamiltonian[37]

$$H = H_0 + \lambda H_{\mathrm{MS}}, \tag{12}$$

where $\lambda = (\frac{1}{M} - \frac{1}{M'})$. For a small amount of λ, the nuclear recoil contribution can be expanded in powers of λ:[38]

$$E_{\mathrm{MS}}(\lambda) = E_{\mathrm{MS}}^{(0)} + E_{\mathrm{MS}}^{(1)}\lambda + \sum_{k=2}^{\infty} E_{\mathrm{MS}}^{(k)}\lambda^k, \tag{13}$$

where

$$E_{\mathrm{MS}}^{(k)} = \frac{1}{k!}\frac{\mathrm{d}^k}{\mathrm{d}\lambda^k}E_{\mathrm{MS}}(\lambda)_{|\lambda=0}. \tag{14}$$

The coefficient $E_{\mathrm{MS}}^{(1)}$ corresponds to the contribution of the order $1/Z$ to the relativistic nuclear recoil correction. Therefore, by keeping the first-order terms and ignoring the higher-order terms, we obtain

$$k_{\mathrm{NMS}} = \lim_{\lambda\to 0}\frac{\mathrm{d}E_{\mathrm{NMS}}}{\mathrm{d}\lambda}, \tag{15}$$

$$k_{\mathrm{SMS}} = \lim_{\lambda\to 0}\frac{\mathrm{d}E_{\mathrm{SMS}}}{\mathrm{d}\lambda}. \tag{16}$$

The field shift factor F can be calculated using the same approach.

Table 4 presents a detailed comparison of the $K_{i,\mathrm{NMS}}$, $K_{i,\mathrm{SMS}}$, $K_{i,\mathrm{MS}}$, and F_i obtained using the RIS4 program and the finite-field method. The labels "MCDHF" and "finite-field" denote the respective computational approaches. Δ represents the difference between the finite-field method and the RIS calculations, which serves as a quantitative measure of the consistency between the two approaches. It is evident that the results obtained from both methods show excellent agreement. The largest discrepancy in the field shift, observed for the transition $2s\ ^2S_{1/2} \rightarrow 2p\ ^2P_{1/2}$, is only 1.61×10^3 GHz/fm^2, corresponding to a relative difference of approximately 1%. Moreover, the relative difference for $K_{i,\mathrm{NMS}}$ is less than 1%, while that for $K_{i,\mathrm{SMS}}$ is below 0.01%. These findings demonstrate the high reliability and consistency of the isotope shift factors calculated using both methods, which is crucial for advancing our understanding of isotope shifts. This comparative analysis not only validates the accuracy of both methods but also highlights their applicability to high-precision studies in atomic physics, such as the determination of isotope shifts and the evaluation of nuclear charge distributions.

Table 4. Comparison of the values of $K_{i,\mathrm{NMS}}$, $K_{i,\mathrm{SMS}}$, $K_{i,\mathrm{MS}}$ (in 10^3 GHz u), and F_i (in 10^3 GHz/fm^2) for the transitions $1s^22s\ ^2S_{1/2} \rightarrow 1s^22p\ ^2P_{1/2,3/2}$ obtained using two different calculation methods. Notably, the calculation of the MS parameter does not incorporate the contribution of the QED effect to the nuclear recoil operator.

	$1s^22s\ ^2S_{1/2} \rightarrow 1s^22p\ ^2P_{1/2}$			$1s^22s\ ^2S_{1/2} \rightarrow 1s^22p\ ^2P_{3/2}$		
	MCDHF	Finite-field	Δ	MCDHF	Finite-field	Δ
ΔK_{NMS}	172.25	170.71	−1.54	−263.37	−264.48	−1.11
ΔK_{SMS}	−1001.33	−1001.26	0.07	−1701.58	−1701.42	0.16
ΔK_{MS}	−829.08	−830.55	−1.47	−1964.95	−1965.90	−0.95
ΔF	−136.98	−138.51	−1.53	−156.21	−157.82	−1.61

3.4. Isotope shift

Table 5 presents the MS, FS, and IS (in meV) results for the $2s\ ^2S_{1/2} \rightarrow 2p\ ^2P_{1/2,3/2}$ transitions of Li-like $^{A,232}Th^{87+}$ ions (where A = 227, 228, 229, 230) using the MCDHF method. It can be seen that the isotope shift of thorium mainly comes from the field shift, while the contribution from the MS is less than 1%. This is due to the fact that as the atomic number increases, the MSs can be regarded as constants, but the

field shifts increase drastically and become dominant at high Z.

Table 5. Values of MS, FS, and IS (in meV) for the $2s\ ^2S_{1/2} \rightarrow 2p\ ^2P_{1/2,3/2}$ transitions of Li-like $^{A,232}Th^{87+}$ ions. The $\delta\langle r^2\rangle$ value was adopted from Ref. [39]. Note: FS = field shift; IS = isotope shift.

	$1s^22s\ ^2S_{1/2} \rightarrow 1s^22p\ ^2P_{1/2}$			$1s^22s\ ^2S_{1/2} \rightarrow 1s^22p\ ^2P_{3/2}$		
	MS	FS	IS	MS	FS	IS
$^{232,227}Th^{87+}$	1.34	286.63	287.97	1.73	319.36	321.09
$^{232,228}Th^{87+}$	1.07	233.03	234.10	1.38	259.64	261.01
$^{232,229}Th^{87+}$	0.80	188.45	189.25	1.03	209.97	211.00
$^{232,230}Th^{87+}$	0.53	115.67	116.20	0.68	128.87	129.56
			111.90[13]			123.90[13]

4. Conclusions

In summary, the transition energies of the $1s^22s\ ^2S_{1/2} \rightarrow 1s^22p\ ^2P_{1/2,3/2}$ transitions in Li-like Th^{87+} ions were calculated using the MCDHF method and the model-QED method. The mass and field shifts of Li-like Th^{87+} ions were calculated using two different methods, namely, the MCDHF and finite-field methods. It was found that these two methods exhibit good consistency, particularly as the relative difference for $K_{i,\mathrm{NMS}}$ was less than 0.01%. Our results agree very well with Zubova *et al.*'s calculation.[13] Finally, the isotope shift due to $2s\ ^2S_{1/2} \rightarrow 2p\ ^2P_{1/2,3/2}$ transitions in Li-like Th^{87+} ions was presented. The results show that as the mass number increases, the isotope shift gradually decreases. The total isotope shifts of thorium mainly originate from the field shifts, while the contribution from the MSs is less than 1%. This work provides theoretical support for testing QED effects in highly charged ions and offers data grounded in theory for measuring the nuclear charge radius of thorium ions.

Acknowledgments

Project supported by the National Key Research and Development Program of China (Grant No. 2022YFA1602500), the National Natural Science Foundation of China (Grant Nos. 1236040286, 12474250, 12174316, 12464036, and 12404306), the Young Teachers Scientific Research Ability Promotion Plan of Northwest Normal University (Grant No. NWNU-LKQN2020-10), and the Funds for Innovative Fundamental Research Group Project of Gansu Province (Grant No. 20JR5RA541).

References

[1] Zubova N, Anisimova I, Kaygorodov M Y, Kozhedub Y S, Malyshev A, Shabaev V, Tupitsyn I, Plunien G, Brandau C and Stöhlker T 2019 *J. Phys. B: At. Mol. Opt. Phys.* **52** 185001
[2] Orts R S, Harman Z, López-Urrutia J C, Artemyev A N, Bruhns H, Martínez A G, Jentschura U D, Keitel C H, Lapierre A, Mironov V, *et al.* 2006 *Phys. Rev. Lett.* **97** 103002
[3] Brandau C, Kozhuharov C, Harman Z, Müller A, Schippers S, Kozhedub Y, Bernhardt D, Böhm S, Jacobi J, Schmidt E W, *et al.* 2008 *Phys. Rev. Lett.* **100** 073201
[4] Silwal R, Lapierre A, Gillaspy J D, Dreiling J M, Blundell S, Borovik Jr A, Gwinner G, Villari A, Ralchenko Y, Takacs E, *et al.* 2018 *Phys. Rev. A* **98** 052502
[5] Silwal R, Lapierre A, Gillaspy J, Dreiling J, Blundell S, Borovik Jr A, Gwinner G, Villari A, Ralchenko Y, Takacs E, *et al.* 2020 *Phys. Rev. A* **101** 062512
[6] Hosier A, Blundell S, Silwal R, Lapierre A, Gillaspy J, Gwinner G, Tan J, Kwiatkowski A, Wang Y, Staiger H, *et al.* 2024 *J. Phys. B: At. Mol. Opt. Phys.* **57** 195001
[7] Scharl K, Ding S, Holthoff G, Hussain M I, Kraemer S, Löbell L, Moritz D, Rozibakieva T, Seiferle B, Zacherl F, *et al.* 2023 *Atoms* **11** 108
[8] Kraemer S, Chhetri P, Bara S, Claessens A, De Witte H, Elskens Y, Ferrer R, Kudryavtsev Y, Sels S, Van Den Bergh P, *et al.* 2023 *Nucl. Instr. Meth. in Phys. Res. B* **542** 1
[9] Beloy K 2023 *Phys. Rev. Lett.* **130** 103201
[10] Yamaguchi A, Shigekawa Y, Haba H, Wada M and Katori H 2024 *J. Phys. Conf. Ser.* **2889** 012041
[11] Zhang C, Ooi T, Higgins J S, Doyle J F, von der Wense L, Beeks K, Leitner A, Kazakov G A, Li P, Thirolf P G, *et al.* 2024 *Nature* **633** 63
[12] Yamaguchi A, Shigekawa Y, Haba H, Kikunaga H, Shirasaki K, Wada M and Katori H 2024 *Nature* **629** 62
[13] Zubova N, Kozhedub Y, Shabaev V, Tupitsyn I, Volotka A, Plunien G, Brandau C and Stöhlker T 2014 *Phys. Rev. A* **90** 062512
[14] Li J, Nazé C, Godefroid M, Fritzsche S, Gaigalas G, Indelicato P and Jönsson P 2012 *Phys. Rev. A* **86** 022518
[15] Fischer C F, Gaigalas G, Jönsson P and Bieroń J 2019 *Comput. Phys. Commun.* **237** 184
[16] Jönsson P, Gaigalas G, Fischer C F, Bieroń J, Grant I P, Brage T, Ekman J, Godefroid M, Grumer J, Li J, *et al.* 2023 *Atoms* **11** 68
[17] Li B B, Jiang J, Wu L, Zhang R K, Li X J and Dong C Z 2024 *J. Phys. B: At. Mol. Opt. Phys.* **57** 115003
[18] Shabaev V, Tupitsyn I and Yerokhin V 2015 *Comput. Phys. Commun.* **189** 175
[19] Shabaev V, Tupitsyn I and Yerokhin V 2013 *Phys. Rev. A* **88** 012513
[20] Grant I P 2007 *Relativistic quantum theory of atoms and molecules: theory and computation* (Springer)
[21] Fischer C F, Godefroid M, Brage T, Jönsson P and Gaigalas G 2016 *J. Phys. B: At. Mol. Opt. Phys.* **49** 182004
[22] Jönsson P, Godefroid M, Gaigalas G, Ekman J, Grumer J, Li W, Li J, Brage T, Grant I P, Bieroń J, *et al.* 2022 *Atoms* **11** 7
[23] Palmer C 1987 *J. Phys. B: At. Mol. Opt. Phys.* **20** 5987
[24] Shabaev V and Artemyev A 1994 *J. Phys. B: At. Mol. Opt. Phys.* **27** 1307
[25] Shabaev V 1998 *Phys. Rev. A* **57** 59
[26] Gaidamauskas E, Nazé C, Rynkun P, Gaigalas G, Jönsson P and Godefroid M 2011 *J. Phys. B: At. Mol. Opt. Phys.* **44** 175003
[27] Torbohm G, Fricke B and Rosén A 1985 *Phys. Rev. A* **31** 2038
[28] Chen M, Cheng K, Johnson W and Sapirstein J 1995 *Phys. Rev. A* **52** 266
[29] Cheng K, Chen M and Sapirstein J 2000 *Phys. Rev. A* **62** 054501
[30] Yerokhin V, Artemyev A, Shabaev V, Sysak M, Zherebtsov O and Soff G 2001 *Phys. Rev. A* **64** 032109
[31] Blundell S A 1993 *Phys. Rev. A* **47** 1790
[32] Sapirstein J and Cheng K 2011 *Phys. Rev. A* **83** 012504
[33] Zhang H L, Sampson D H and Fontes C J 1990 *Atomic Data and Nuclear Data Tables* **44** 31
[34] Beiersdorfer P, Osterheld A, Elliott S, Chen M, Knapp D and Reed K 1995 *Phys. Rev. A* **52** 2693
[35] Ekman J, Jönsson P, Godefroid M, Nazé C, Gaigalas G and Bieroń J 2019 *Comput. Phys. Commun.* **235** 433
[36] Kozhedub Y, Volotka A, Artemyev A, Glazov D, Plunien G, Shabaev V, Tupitsyn I and Stöhlker T 2010 *Phys. Rev. A* **81** 042513
[37] Berengut J C, Flambaum V V and Kozlov M G 2005 *Phys. Rev. A* **72** 044501
[38] Zubova N A, Malyshev A V, Tupitsyn I I, Shabaev V M, Kozhedub Y S, Plunien G, Brandau C and Stöhlker T 2016 *Phys. Rev. A* **93** 052502
[39] Angeli I and Marinova K P 2013 *Atomic Data and Nuclear Data Tables* **99** 69